Nat. Volatiles & Essent. Oils, 2021; 8(4): 13684-13695

NVEO
Natural Volatiles &
Essential Oils

Light Fractionation Consents For Enhancement Of Photodynamic Therapy In Streptococcus Mutes Biofilm

AMMAR ABDULAMEER AZEEZ[1] , QUDAMA ABDULAMEER AZEEZ[2]

[1]Directorate of education in diyala, Iraq

[2]Directorate of education in diyala, Iraq

Abstract: Microbial infections continue to be a major cause of death. The culprit is biofilm that forms multiple drug-resistant strains of bacteria. Biofilms are the three-dimensional, surface-attached structure of heteromorphic microorganisms embedded in extracellular polymeric substances (EPS). The main antibiotic resistance mechanisms in biofilm-associated bacteria are antibiotic penetration, efflux and production. They prevent drug access to the cell's interior. To avoid the severe biofilm-related infections, it is urgent to look into novel treatments like photodynamic therapy (PDT).This study was initiated to examine the photo-inactivation efficiency and effect of reactive oxygen substances (ROS) on Gram positive and negative bacterial cells as well as their biofilm. Each dye was photo activated at a 10uM level using 630nm laser light. This light was used to kill Klebsiella pneumoniae and Enterococcus foecalis. E. faecalis showed a reduction of 8log10 bacterial counts, while K. pneumoniae saw a reduction of 3log10. Photodynamic inhibition was more prominent in Gram positive bacteria, according to antibiofilm and extracellular polysaccharides reduction assay.This was in addition to the results of confocal laser microscopy, (CLSM), and scanning electron microscopywhich showed an increase of cell permeability of propionidium iodide in cells. Also, there was a leakage of cellular constituents within preformed biofilm that had been treated with photodynamic therapy. This is a reflection of the antibiofilm effect of photodynamic treatment. The increased ROS production in Gram positive bacteria cells was confirmed by fluorescence spectroscopic analysis. Results showed that Gram positive bacteria (E.faecalis), are more vulnerable to PDT because of increased ROS generation, higher photosensitizer binding efficacy and DNA degradation. The efficacy of phenothiazinium dyes against planktonic as well as biofilm cells has been proven. We conclude that Gram positive bacteria (Enterococcus foecalis) are more vulnerable to APDT because of higher ROS generation, increased photosensitizer binding efficacy and DNA degradation. The efficacy of phenothiazinium dyes against planktonic as well as biofilm cells has been proven.

Keywords: Biofilm; DCFH-DA; DNA fragmentation; Gram negative; Gram positive; Photodynamic therapy.

I. Introduction

There are many genetically different organisms in the microbial ecosystem of the human mouth. Streptococcus Mutans, a member the oral microflora, is considered to be the primary causative agent for dental caries. This is a multifactorial chronic infection that causes irreversible tooth decay. S. mutans is a major contributor to biofilm in the human oral flora. Biofilms are three-dimensional, surface-attached structures made up of heteromorphic microorganisms and embedded in self-generated molecular plastic materials. Biofilms are composed of EPS. It acts as a physical barrier, and increases resistance to antimicrobial agents. Infective endocarditis is also a result of the biofilm produced by this bacterium. This can cause death and morbidity of up to 50%, even with antibiotic treatment.PDT was developed as a novel process to combat biofilm-related infections. This is due to the severe nature of these infections. PDT uses a non-toxic and light sensitive dye, called photosensitizer. In the presence of oxygen rich environments, harmless visible light with the appropriate wavelength produces a phototoxic reaction. A PS is excited by light and can be converted to an excited electronic singlet state. This state reacts with ground state oxygen in two ways. Intersystem crossing allows it to reach its long-lasting excited triplet state. 2012. Type I reactions involve the transfer of electrons or hydrogen atoms from the triplet states PS to a substrate. This leads to the formation of radical's derived water.These radicals can react with molecular oxygen to create free radicals such as hydrogen peroxide and hydroxyl radicals. This can lead to lipid peroxidation and cellular damage, and even death. Type II reactions involve energy transfer between the triplet state PS and molecular oxygen to create excited singlet-state oxygen. This reactive species can react with the cell's biomolecules such as nucleic acids and phospholipids and cause the cell to be destroyed. Both reactions can occur simultaneously, but the ratio depends on the PS used and the microenvironment in which the PS is located. A few photosensitizers can produce singlet oxygen as well as free radicals. The synergistic effects of ROS produced by PS were also proposed in an earlier study. It is known that PDT can be used to inactivate any known class of microorganisms both in vitro and in vivo. This includes Gram-negative bacteria, fungi and viruses.Additionally, photo inactivation of microorganisms is fast (many logs were killed in less than a minute), compared to antibiotics which can take many days or even weeks to work. This could lead to drug resistance, but it is still not reported.

Many studies have shown that nanoparticles can be used to enhance antimicrobial PDT [Khan and al. 2012], salts [St Denis et al. 2013], antibiotics etc. It is important to note that the addition of these materials could pose a threat to mammalian cells. In-vivo experiments can raise serious concerns about toxicity. It is important to note that antibacterial PDT could not be potentiated by adding aforementioned materials clinically without testing its harmful effects. These are the major concerns

that prompted our research to enhance photodynamic therapy and decrease light irradiation times by fractionating the used light dose with phenothiazinium, a photosensitizer.

II. Materials and Methods

Human serum albumin (HSA), human insulin, thioflavin T (ThT), 1-anilino 8- naphthalene sulfonate (ANS), and ibuprofen (IBFN) were procured from Sigma Aldrich, India. All other reagents used were of analytical grade.

Sample preparation

A stock solution of HSA was made by dissolving protein in 20 mM phosphate buffer, pH 7.4 and extensively dialyzed against the same buffer. Experiments were carried out using double distilled water. Protein concentration was determined spectrophotometrically using = 5.3 at 280 nm. HSA fibrils were prepared by incubating HSA at 65°C for 120 h, in sodium phosphate buffer (pH 7.4). Stock solution of insulin was prepared by dissolving insulin lyophilized powder in 50 mM Gly-HCl buffer, pH 2.0, and insulin concentration was determined by measuring absorbance at 276 nm, with the extinction coefficients of 1.0 for 1 mg ml-1. Fibrils were prepared by incubating insulin solution at 65°C for 72 h.

Thioflavin T staining

The aggregation of protein was determined by ThT fluorescence assay performed on Shimadzu fluorescence spectrophotometer (RF-5301 PC). ThT solution (5000μM) was prepared in double distilled water and filtered with 0.45 micron Millipore filter. Samples of HSA with or without IBFN (incubated at 65°C for 120 h, pH 7.4) were taken at definite time interval and mixed with ThT to achieve a final ThT concentration of 40 μM. Samples were incubated in dark for 30 minutes. The excitation wavelength was 440 nm and ThT fluorescence intensity was recorded at 481 nm. The excitation and emission slit widths were set at 5 and 3 nm, respectively. Sodium phosphate buffer 20 mM (pH 7.4) was used for dilution, and spectra were corrected for respective blanks. For insulin, samples, incubated with or without IBFN, were withdrawn at definite time interval and mixed with ThT to have the final protein and dye concentration of 20 μM. Buffer (pH 2.0) was used for dilution, and spectrawere corrected for the respective blanks. All measurements were performed in triplicates.

Congo red binding assay

The Congo red (CR) absorbance (400–650 nm) spectra were measured on UV–vis spectrophotometer (Perkin Elmer Lambda 25) in a 1 cm path length cuvette. Congo red was dissolved in a 20 mM phosphate buffer (pH 7.4) and filtered through 0.45 μm membrane filter. The concentration of Congo red was determined using εM of 45,000 M −1 cm−1 at 498 nm. In Congo red experiments, the

protein concentration was fixed at 40 µM. Congo red was mixed at a molar ratio of 1:1 with protein in the absence and presence of varying concentration of IBFN (incubated for 120 h at 65°C) and kept for 30 min in dark.

ANS binding assay

ANS fluorescence was recorded on spectrophotometer (RF-5301 PC) with excitation wavelength of 380 nm, and emission intensity was recorded at 465 nm. HSA samples with and without IBFN were mixed with 20 fold molar excess of ANS and then mixtures were kept in dark for 30 minutes at room temperature. Protein concentration was fixed at 40 µM. All measurements were performed in triplicates.

Circular dichroism measurements

To monitor the secondary and tertiary structural change of protein during aggregation, CD spectra were collected in far- (200-250 nm) and near -UV (250-350 nm) range on a JASCO J-815 Spectropolarimeter with a thermostatically controlled cell holder attached to a Peltier heat pump with MultiTech water circulator. The experiments were carried out with HSA samples in absence and presence of IBFN in molar ratio of 1:0, 1:12.5 and 1:25. For the far-UV CD analyses, solutions contained 10 µM HSA, whereas solutions with 40 µM HSA were used for near UV-CD experiments.

Eradication of planktonic bacteria

Plate count was used to evaluate antimicrobial photodynamic therapy containing 10uM of TBO, AAA and NMB. TBO, AA, and NMB caused a decrease in viability of S. mutans cell viability by 6-6.5 log10 when photoinactivated with 5 J/cm2 fractionated light compared to 4.5 logged10 continuous light.

Quantification of biofilm reduction

Preliminary investigations using crystal violet assay were done to determine the antibiofilm inhibition of TBO and AA. Each dye inhibits biofilm formation in 49%, 50%, and 27% respectively when given continuous light doses at 5 J/cm2. However, 57%, 62%, and 55% can be achieved by fractionating the light dose, as shown in Figure 1.

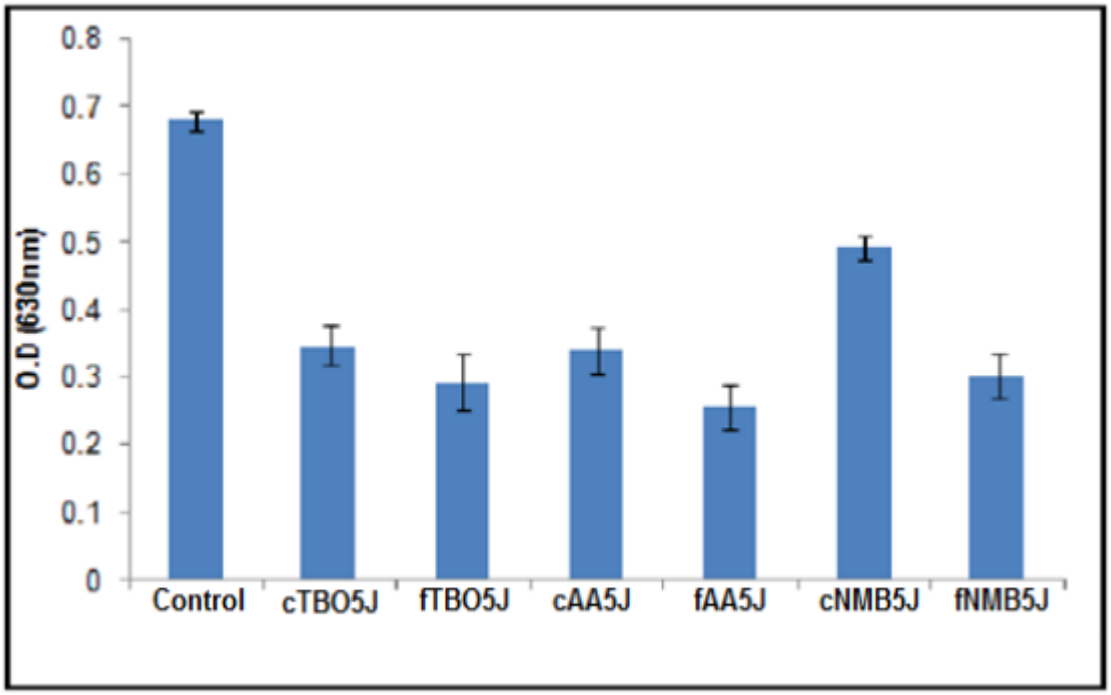

Figure 1: The effect of lycopene on continuous and dissociated light radiation on the formation of biofilm

Assessment of cellular viability

The conversion amount of XTT indicates the microorganisms' metabolic activity in the biofilm following PDT treatment. After treatment with TBO and AA at a 10 uM concentration and continuous light doses of 96%, 84%, 90%, and 96%, respectively, viable cells were found. After fractionating light doses, the viability of S.mutans was 62%, 69%, and 81%, respectively

Reduction in EPS formation

The structure, spread and maintenance of the EPS formation biofilm is crucial. CR binding assay is used to analyse EPS product. This is directly related to the EPS number generated after the PDT. EPS output was reduced by 10% TBO, AAA, and NMB and 5J / cm2 continuous light dose by 30%, 18% and 10%, respectively. However, 36%, 30%, and 14% were achieved, respectively, when the photo was inactivated at light doses by the same energy fragmentation pieces.

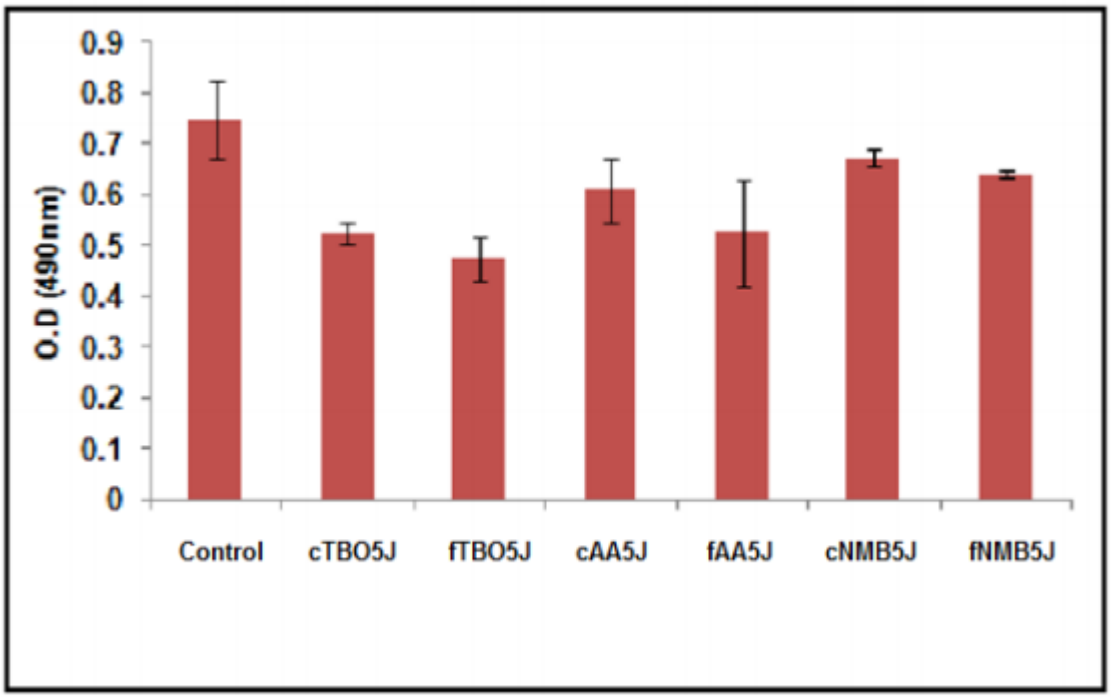

Figure 2: Light irradiation on EPS reduction

Biofilm reduction by PDT

Below figure shows the antibiofilm effects photosensitization of TBO and AA on matured biofilm viability. Biofilms exposed to 50 uM of each PS, and then to 50 J/cm2 continuous light doses showed a significant 3.6-4.2 log10 decrease in bacterial viability. Photoinactivation rates were higher with fractionated light than with continuous light doses. After applying 100 J/cm2 light dose, 100% of the matured biofilm of S.mutans was reduced.

Effect of PDT on S. mutans biofilm architecture visualized by SEM

SEM was used to examine the overall morphology and cell structure of the biofilm cells after PDT. The cells of the control are embedded in an EP matrix which accelerates cell clustering. Biofilms were reduced by irradiating them with a sub-MIC level of TBO, AA, and NMB. Biofilms treated with fractionated sunlight showed a remarkable decrease in the number of adherent bacteria. The cells were completely ruptured and had an irregular shape. Leakage of cellular constituents was also observed. Figure 3 shows that most bacteria was either single-cell or in short chains.

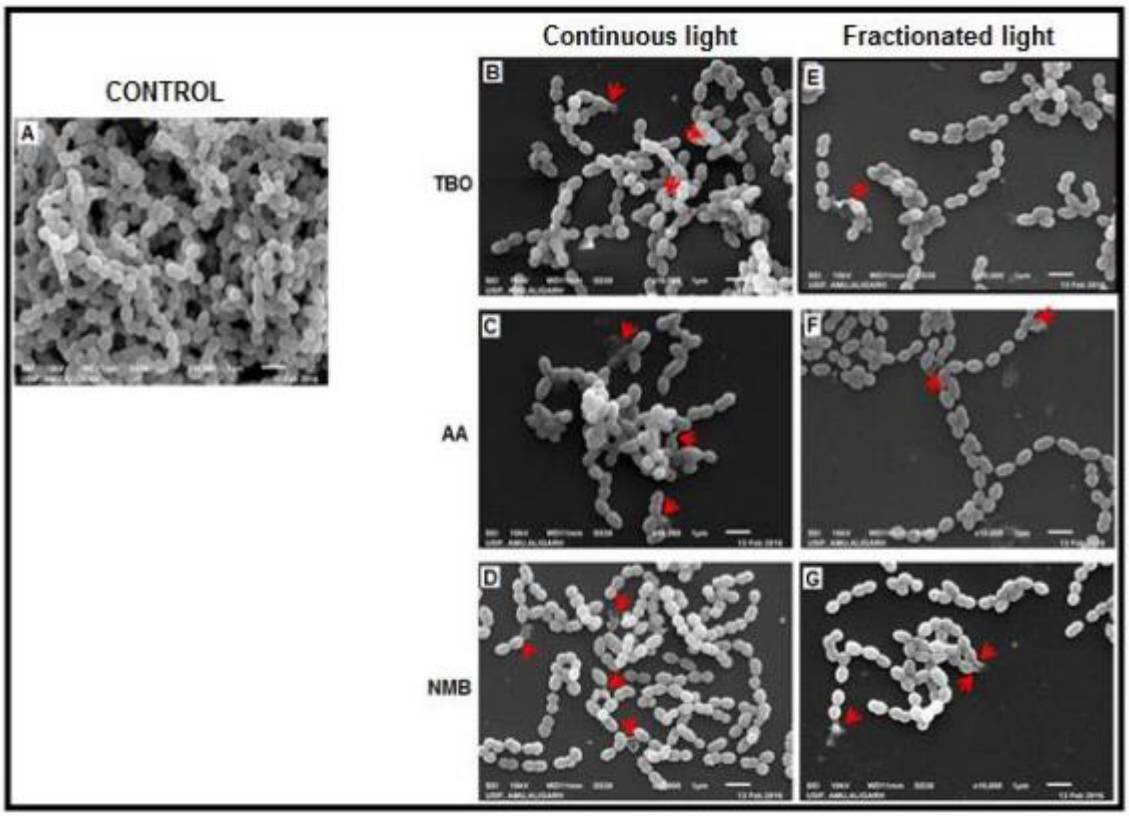

Figure 3: Biofilm architecture shows effect of PDT

Intracellular ROS production discovery

S. mutans was exposed with PDT using 10uM TBO and AA. Figure 5.8a shows an increase in fluorescence. Comparing cells untreated (control), we observed a 10.8 and 8.7 fold increase in fluorescence in cells that were treated with TBO or AA with continuous 5J/cm2 light. Further fluorescence was seen at 13, 12, and 11 fold respectively when cells were treated with fractionated light doses (5 J/cm2) of 5 J/cm2. It was shown that TBO produced higher ROS levels than NMB or AA.

Effect of quenchers on ROS production

Specific quencher was used to determine the relative contributions of singlet oxygen (Type 2) and free radical species (1 Type I). Figure 5.8b shows a reduction in DCF fluorescence intensity when DMT was present (Figure 5.8b). These results indicated the presence of *OH radicals that were quenched with free radical scavenger DMT.

Type I (•OH) ROS detection

We use HPF fluorescence probes to measure the radicals produced by radiation with TBO, AA, and NMB in the presence of continuous or dissociated light doses of *OH. It further supports the production of type I ROS in cells. These data showed TBO, AA and NMB generated most *OH

radicals. This further enhanced fractionating given dose. NMB produces three more of those remaining OH radicals.

Type II singlet oxygen ($_1O^2$) quantum yield

TBO, NMB and AA were also measured in PBS to determine their singlet oxygen production capabilities. This was done by measuring the AMDA degradation rate. Each phenothiazinium colour dye exhibits the singlet-oxygen quantum yield in aqueous solutions, but singlet oxygen quantum yields were increased after fractionating the applied dose (Figure 5.8d). TBO had a lower singlet oxygen generation capability than NMB, which is likely due to NMB's lower water solubility and therefore higher aggregation.

RT-PCR profile for Gene-Expression

All tested genes showed significant up-regulation, indicating the importance of PDT in heat shock reactions, oxidative stress and metabolic pathway as well as in the repair mechanism and mRNA degrading.

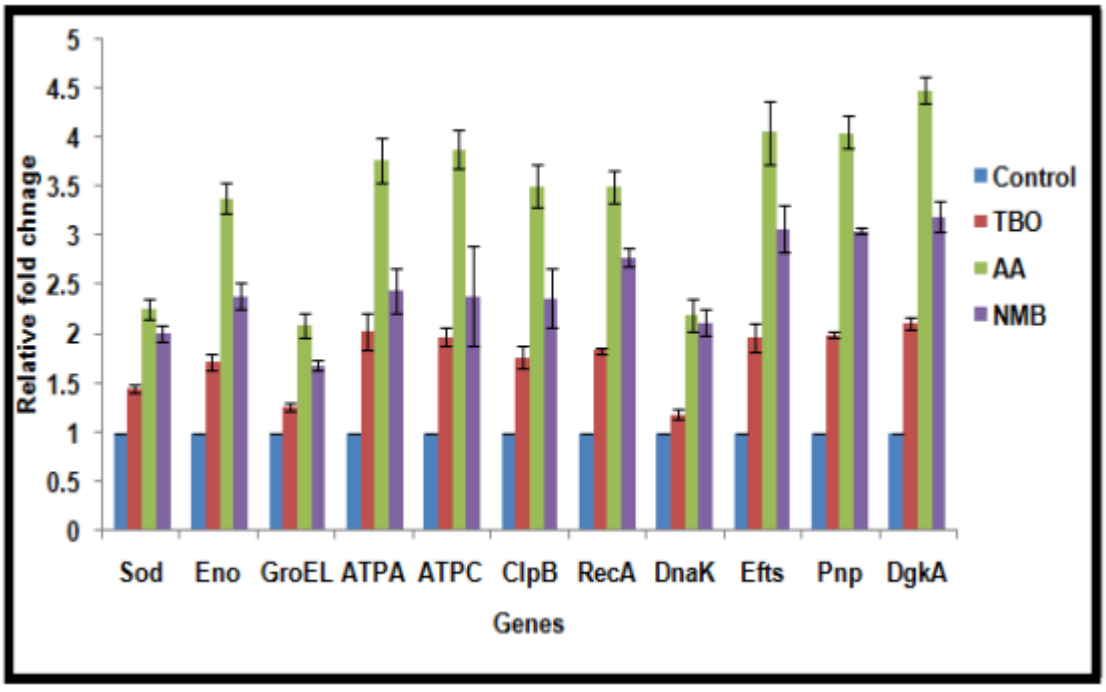

Figure 4: PDT with TBO and AA in combination with light radiation and control was used to analyse the expression profiles of several genes in S. mutans biofilm.

Protein network analysis

To evaluate the interactions between differentially expressed proteins, protein interaction networks were created. Figure 5.10 shows that all of the proteins interacted with one another (Figure 5). The closed web was predicted by the protein of the genes that showed upregulation under qPCR.

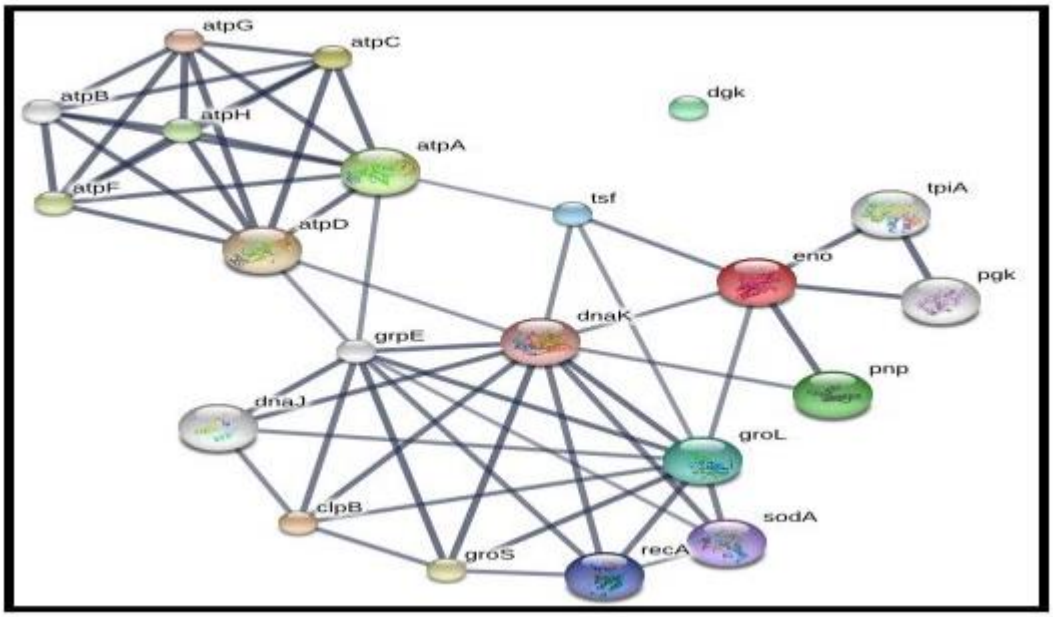

Figure 5: Protein-protein interaction through STRING.

MTT assay was used to determine the cytotoxic effects of TBO, AA, and NMB. These PS did not have a significant impact on cell viability in HEK-293 cells. TBO, NMB and AA showed viability of more than 60% at concentrations higher than those used in antibiofilm experiments.

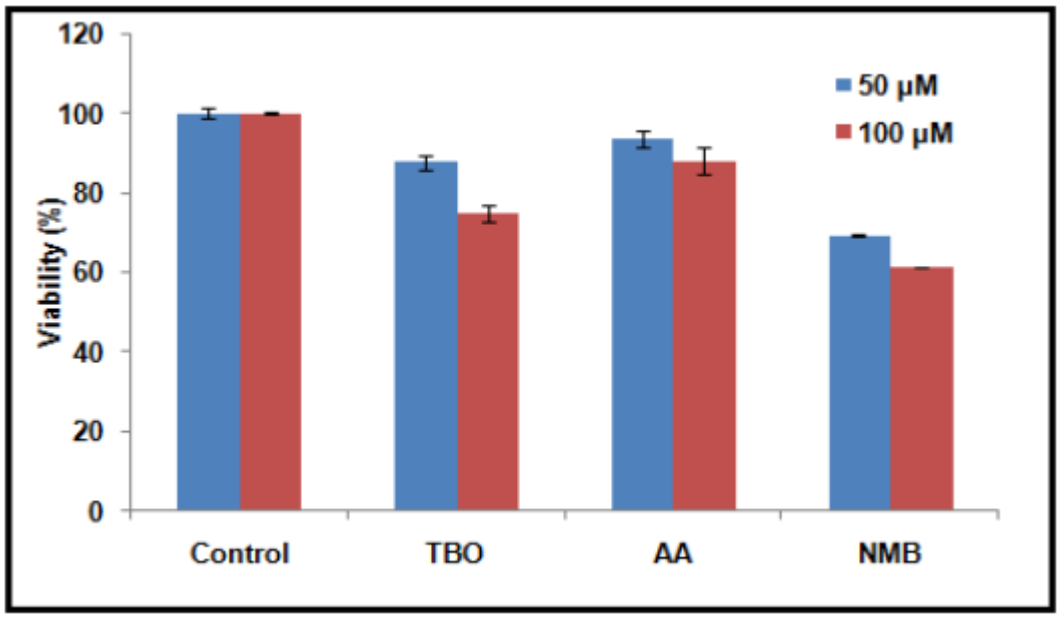

Figure 6: In vitro cytotoxicity assay (MTT) on the HEK-293 cell line.

III. Experimental evaluation and discussion

One of our earlier studies showed that toluidine-blue Osilver nanoparticles (TBOSNP) conjugate enhanced PDT effects on S. Mutans biofilm [Misba and al. 2016. This study was motivated by the

hypothesis that continuous light applied to bacteria cells causes stagnancy in photoinactivation. It could be due to a decrease in target molecules, such as oxygen, or photobleaching of a PS. There is also the possibility that the PS may be replenished or redistributed during the dark period [de Souza and al. 2016. This study shows that fractionating the light dose applied during PDT of S.mutans biofilm in vitro using phenothiazinium dyes (TBO and AA) results in higher cell killing than continuous light.The primary focus of this study was to improve the antibacterial/antibiofilm efficacy of PDT by fractionating the applied light doses. There is evidence that PS activity increases when the applied light dose is fractionated in cancer research, but there are not many reports on bacterial inhibition [Pogue et al. 2008 This is the first time that we have fractionated the light from S. mutans to enhance the antibacterial and biofilm effects of TBO, AAA, and NMB. We also investigated the possibility that fractionating the light dose could cause more photoinhibition and the reaction mechanism. Phenothiazinium dye was chosen because it absorbs light in the red region, which is within visible light range. It also has a high penetration power. It is also water-soluble, positively charged and does not cause toxicity.

Fractionated light is more effective than continuous light for antimicrobial photodynamic inhibition. After being exposed to 5 J/cm2 continuous light with each dye, a 4.5 log10 decrease in the bacterial count of S.mutans was observed. This reduction was increased to 6.5 log10 when the fractionated light dose was applied. The Kasimova et. Kasimova et doesn't support the antimicrobial photodynamic efficacy to inactivate Gram-positive bacteria using continuous lighting. 2014, i.e. It is different from other reports. Log10: 4-5 3log10 [Rolim et al. 2012. These variations could be caused by differences in light dose, concentration, and experimental conditions. This study used 10uM dye concentrations, and a low dose of 5 J/cm2 light. This is in contrast to the 163.5uM and 24 J/cm2 levels for the previous study. Our results were better than those in the previous reports. Light fractionation can further enhance these results.

It was determined that the human embryonic kidney cell line is toxic. Concentrations toxic to S.mutans biofilm weren't found to be toxic. After 24 hours of incubation, cell viability was >50% even at higher levels of TBO, NMB and AA. These data indicate the potential use of these dyes to combat bacteria and biofilm. The concentration used to kill the microbe 7log10 is not reported to have any effect on the genotoxicity of mammalian Keratinocytes. These dyes have low toxicity and photodynamic inhibition on human cells, which indicates their potential for in-vivo use.

IV. Conclusion

The amount of ROS generated upon irradiation is directly related to photodynamic efficiency. This ROS can be further enhanced by fractionating light doses into short pulses. Photochemical

mechanisms involve both singlet oxygen and hydroxyl radical generation, which results in enhanced antibacterial and biofilm efficacy for phenothiazinium-based dyes. This opens up new possibilities for exploring the clinical implications of PDT phenothiazinium dye-mediated PDT with light fractionation. It is possible to reduce the time required to irradiate a PS to a level that is clinically acceptable.

V. References

[1]. Abranches J, Miller JH, Martinez AR, Simpson-Haidaris PJ, Burne RA, Lemos JA. The collagen-binding protein Cnm is required for Streptococcus mutans adherence to and intracellular invasion of human coronary artery endothelial cells. Infect. immun. 2011; 79:2277-84.

[2]. Achtman M, Wagner M. Microbial diversity and the genetic nature of microbial species. Nature Rev. Microbiol. 2008; 6: 431-40.

[3]. Ackroyd R, Kelty C, Brown N, Reed M. The history of photodetection and photodynamic therapy. Photochemistry and photobiology. 2001; 74; 656-669.

[4]. Al-Ahmad A, Tennert C, Karygianni L, Wrbas KT, Hellwig E, Altenburger MJ. Antimicrobial photodynamic therapy using visible light plus water-filtered infrared-A (wIRA). Journal of Medical Microbiology. 2013; 62:467–473.

[5]. Bakkiyaraj D, Pandian SK. In vitro and in vivo antibiofilm activity of a coral associated actinomycete against drug resistant Staphylococcus aureus biofilms. Biofouling. 2010; 26: 711–717

[6]. Bankura KP, Maity D, Mollick MMR, Mondal D, Bhowmick B, Bain MK, Chakraborty A, Sarkar J, Acharya K, Chattopadhyay D. Synthesis, characterization and antimicrobial activity of dextran stabilized silver nanoparticles in aqueous medium. Carbohyd Polym.2012; 89: 1159– 1165.

[7]. Barraud N, Schleheck D, Klebensberger J, Webb JS, Hassett DJ, Rice SA, KjellebergS.Nitric oxide signaling in Pseudomonas aeruginosa biofilms mediates phosphodiesterase activity, decreased cyclic di-GMP levels, and enhanced dispersal. J Bacteriol. 2009; 191: 7333-7342.

[8]. Carpenter BL, Situ X, Scholle F, Bartelmess J, Weare WW, Ghiladi RA. Antiviral, Antifungal and Antibacterial Activities of a BODIPY-Based Photosensitizer. Molecules.2015; 20: 10604-10621.

[9]. Chen J, Cesario TC, Rentzepis PM. Rationale and mechanism for the low photoinactivation rate of bacteria in plasma. PNAS. 2014; 111: 33-38.

[10]. Chung PY. The emerging problems of Klebsiella pneumoniae infections: carbapenem resistance and biofilm formation. FEMS Microbiology Letters. 2016; 363: 219.

[11]. Costa L, Faustino MAF, Tomé JPC, Neves MGPS, Tome AC, Cavaleiro JAS, Cunha A, Almeida A. Involvement of type I and type II mechanisms on the photoinactivation of non-enveloped DNA and RNA bacteriophages. J PhotochemPhotobiol B. 2013; 120:10–16.

[12]. Demidova TN, Hamblin MR. Effect of Cell-Photosensitizer Binding and Cell Density on Microbial Photoinactivation. Antimicrob Agents chemother. 2005; 49: 2329–2335.

[13]. Demidova TN, Hamblin MR. Effect of cell-photosensitizer binding and cell density on microbial photoinactivation. Antimicrob Agents Chemother. 2005; 49: 2329-2335.

[14]. Diggikar RS, Patil RH, Kale SB, Thombre DK, Gade WN, Kulkarni MV, Kale BB. Silver-decorated orthorhombic nanotubes of lithium vanadium oxide: an impeder of bacterial growth and biofilm. ApplMicrobiolBiotechnol. 2013; 97: 8283–8290.

[15]. Fux CA, Costerton JW, Stewart PS, Stoodley P. Survival strategies of infectious biofilms. Trends Microbiol. 2005; 13: 34–40.

[16]. A.S. Garcez, S.C. Núnez, N. Azambuja Jr, E.R. Fregnani, H.M. Rodriguez, M.R. Hamblin, H. Suzuki, M.S. Ribeiro, Effects of photodynamic therapy on Gram-positive and Gram-negative bacterial biofilms by bioluminescence imaging and scanning electron microscopic analysis, Photomed. Laser. Surg. 31 (2013) 519-525.

[17]. L. Misba, S. Kulshrestha, A.U. Khan, Antibiofilm action of a toluidine blue O-silver nanoparticle conjugate on Streptococcus mutans: a mechanism of type I photodynamic therapy, Biofouling. 32 (2016) 313-328.

[18]. S. George, A. Kishen, Influence of photosensitizer solvent on the mechanisms of photoactivated killing of Enterococcus faecalis. J. Photochem. Photobiol. B 84 (2008) 734-40.

[19]. C.A. Fux, P. Stoodley, L. Hall-Stoodley, J.W. Costerton, Bacterial biofilms: a diagnostic and therapeutic challenge, Expert. Rev. Anti. Infect. Ther. 1 (2003) 667- 683.

[20]. M. Tanaka, M. Kinoshita, Y. Yoshihara, N. Shinomiya, S. Seki, K. Nemoto, T. Hirayama, T. Dai, L. Huang, M.R. Hamblin, Y. Morimoto, Optimal Photosensitizers for Photodynamic Therapy of Infections Should Kill Bacteria but Spare Neutrophils, PhotochemPhotobiol. B 88 (2012) 227–232.